JOURNAL OF GEOPHYSICAL RESEARCH, VOL. 96, NO. B3, PAGES 4313–4324, MARCH 10, 1991

# Source Mechanism of the 1987 Vatnafjöll Earthquake in South Iceland

INGI TH. BJARNASON

*Lamont-Doherty Geological Observatory and Department of Geological Sciences of Columbia University*
*Palisades, New York*

PÁLL EINARSSON

*Science Institute, University of Iceland, Reykjavík*

The May 25, 1987, Vatnafjöll earthquake occurred on the Mid-Atlantic plate boundary, at a junction between a transform (the South Iceland Seismic Zone) and a spreading segment (the Eastern Volcanic Zone). The South Iceland Seismic Zone has had the most destructive earthquakes in the history of Iceland with average intervals of 80–100 years and estimated maximum magnitudes around 7. The 1987 Vatnafjöll earthquake was the largest earthquake ($m_b = 5.8$; $M_S = 5.8$; $M_w = 5.9$) in south Iceland since the 1912 magnitude 7 earthquake and is the first event sufficiently large to allow a meaningful study of source process in this geologically interesting region. Foreshocks and aftershocks of the Vatnafjöll earthquake were located with relatively good accuracy. They define an elongated N-S epicentral area, 12 km long and 4 km wide with hypocentral depths mostly between 6 and 13 km. We determined centroid source parameters of the Vatnafjöll earthquake by inverting long-period teleseismic $P$ and $SH$ waves. The centroid source mechanism and foreshock and aftershock distribution indicate N-S right-lateral strike-slip faulting on a near-vertical plane. The rupture initiated near the base of the crust and propagated upward along an approximately 10-km-long fault but did not reach the surface. The centroid depth is well constrained and is between 5 and 8 km depth at the 95% confidence level. The seismic moment is $9.1 \times 10^{24}$ dyn cm. The source has relatively short duration of 3 s, which may indicate higher stress drop than global average of earthquakes of this size. The South Iceland Seismic Zone is a 70-km-long E-W striking transform zone between two overlapping rift zones, the Eastern and Western Volcanic Zones. It is characterized by "bookshelf" type of tectonics; that is, there is no surface faulting in the direction of the transform. Instead, N-S right-lateral strike-slip faults are distributed along and perpendicular to the transform zone. The Vatnafjöll earthquake has characteristics of earthquakes in the South Iceland Seismic Zone and is probably not related directly with magmatic activity in the Eastern Volcanic Zone. The transform zone thus extends farther into the rift zone than was previously recognized.

## INTRODUCTION

The Vatnafjöll earthquake of May 25, 1987 ($m_b = 5.8$; $M_S = 5.8$; $M_w = 5.9$), is the largest earthquake to occur in Iceland since 1976. It occurred in an unpopulated area in south Iceland, and damage was only minor. The epicentral area of the event and its foreshocks and aftershocks are within the Eastern Volcanic Zone, where it joins with the South Iceland Seismic Zone (Figure 1). Both zones are parts of the Mid-Atlantic plate boundary that crosses Iceland: the former is a spreading boundary and the latter is a transform-type zone [*Einarsson*, 1986]. The tectonics of this ridge-transform intersection is not well understood. As this area has been relatively quiet seismically for the last few decades, it has not been known how far into the volcanic zone the transform continues.

Plate divergence in the southern part of Iceland is accommodated by two subparallel rift zones, the Western and the Eastern Volcanic Zones. The gap between them is bridged in the south by a transform zone, the South Iceland Seismic Zone, which takes up the transform motion between the Reykjanes Ridge and the Eastern Volcanic Zone (Figure 1). No comparable seismic zone at present links the northern end of the Western Volcanic Zone to the plate boundary in central Iceland. Partly for this reason one can conclude that rifting is dying out in the Western Zone and is being taken over by the Eastern Zone.

The structure of the volcanic zones is characterized by structural units called volcanic systems [*Sæmundsson*, 1974, 1978; *Jakobsson*, 1979]. Each volcanic system consists of a central volcano and a fissure swarm that transects it. Volcanic production is highest in the central volcano of each system, but fissure eruptions may occur out to considerable distance in the fissure swarm area. Frequently, a geothermal field, acidic volcanism, and a caldera structure are associated with the central volcano. One of the volcanic systems identified in south Iceland is the Vatnafjöll system [*Jakobsson*, 1979] (Figure 1). It is identified primarily on the basis of its petrologic characteristics and a clear productivity maximum, which has built up a distinct volcanic edifice. Its fissure swarm is poorly developed, and thermal activity and caldera are absent. No volcanic activity is known in Vatnafjöll in historical time, i.e., the last 1100 years. This is in contrast to the neighboring volcano Hekla, which has erupted at least 17 times in the same time interval [*Grönvold et al.*, 1983].

The South Iceland Seismic Zone crosses the populated lowland in south Iceland from west to east, and extends into the Eastern Volcanic Zone, which has a width of about 60 km at this latitude. This junction is marked by the Hekla, Vatnafjöll, and Torfajökull volcanic systems (Figure 1). The seismic zone has produced numerous destructive



Paper number 90JB00831.
0148-0227/91/90JB-00831$05.00

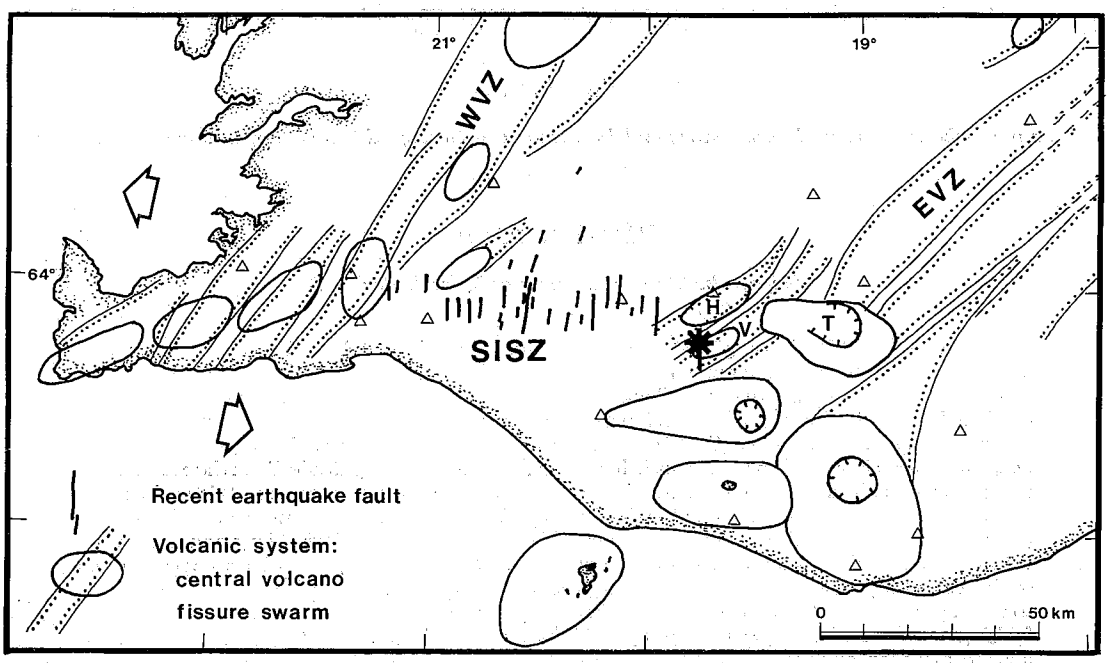


Fig. 1. A tectonic index map of southern Iceland showing the Western and Eastern Volcanic Zones (WVZ, EVZ) and the South Iceland Seismic Zone (SISZ) that connects them near 64°N latitude. The epicenter of the Vatnafjöll earthquake is marked with an asterisk. The arrows show the spreading direction between the Eurasian and North American plates. The full spreading rate is about 2 cm/yr. The Hekla, Vatnafjöll, and Torfajökull central volcanoes are marked with H, V, and T, respectively. Triangles show the locations of seismographs used in this study. Recent earthquake faults and volcanic systems are after *Einarsson and Sæmundsson* [1987].

earthquakes in Icelandic history, some of which have been well documented. It was identified as a transform fault zone by *Ward* [1971], primarily on the basis of its geometric relationship to the ridge system and one poorly constrained fault plane solution that showed strike-slip faulting on an E-W or a N-S striking plane. The spatial and temporal pattern of the seismicity was summarized by *Einarsson et al.* [1981]. The zone is delineated by destruction areas of historical earthquakes, surface ruptures, and instrumentally determined epicenters. It is oriented E-W and is 10–15 km wide. Destruction areas of individual earthquakes and surface faulting show, however, that each event is associated with faulting on N-S striking planes, perpendicular to the trend of the South Iceland Seismic Zone. Destruction areas are elongate in the N-S direction and detailed mapping of surface fractures [*Einarsson and Eiríksson*, 1982] reveal N-S trending arrays of en echelon tension fractures indicating right-lateral faulting. The overall left-lateral transform motion along the zone thus appears to be accommodated by right-lateral faulting on many parallel, transverse faults. *Einarsson and Eiríksson* [1982] speculated that this was an indication of the transient nature of the plate boundary in south Iceland and suggested that the seismic zone was migrating southward in response to propagation of the Eastern Volcanic Zone.

Major earthquake sequences in which most of the zone is affected, tend to last from a few days to about 3 years. These major sequences occur at average intervals of 80–100 years. Each sequence typically begins with a magnitude 7 event in the eastern part of the zone, followed by smaller events farther west. The last sequences occurred in 1732–1734, 1784, and 1896, so the next sequence is expected soon [*Einarsson*, 1985]. In addition to these major sequences, individual large events have occur near the eastern and western ends of the zone, like the magnitude 7 earthquake west of Hekla in 1912.

The Vatnafjöll earthquake in 1987 was the largest event in the South Iceland Seismic Zone since 1912. It immediately raised several important questions: Did it signal renewed magmatic activity of the Vatnafjöll volcanic system? Was it tectonically related to the South Iceland Seismic Zone rather than the volcanic zone? Is it perhaps a prelude to a major sequence of earthquakes in the populated areas in the seismic zone to the west? And what lessons can be learned from it about fracturing of the Icelandic crust?

In this paper we study the faulting mechanism of the Vatnafjöll earthquake in an attempt to answer these questions. Local seismic data are used to locate the event and its foreshocks and aftershocks, and teleseismic, long-period body wave data are used to determine the source mechanism.

## The Earthquake Sequence

The mainshock was accompanied by both foreshocks and aftershocks (Figure 2 and Table 1). Foreshocks began at about 0900 UT May 25, 1987, with a series of five shocks in 3 min, the largest of which was of magnitude 3.8. The foreshock activity was followed by almost 1.5 hours of quiescence. Then there were additional foreshocks, and the main event occurred at 1131 UT. It was immediately followed by numerous aftershocks. The largest one occurred at 1221 UT , and had a magnitude of 3.6. At 1300 UT the activity subsided considerably, but many microearthquakes were still recorded on the closest seismograph, which is near the summit of Hekla at a distance of 10–15 km. Single small

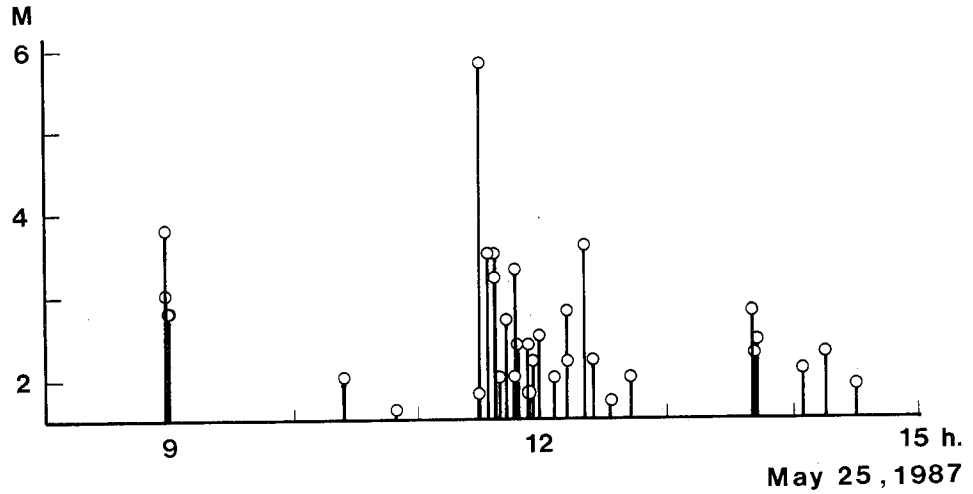


Fig. 2. Magnitudes of earthquakes in the Vatnafjöll sequence as a function of time. The magnitudes are based on the duration of the seismic signal on local seismograms, except for the mainshock, for which $M_S$ is plotted.

TABLE 1. Earthquake Sequence

| Date | Time, UT | Latitude | Longitude | Depth, km | Magnitude | $\Delta h$,[a] km | $\Delta z$,[a] km |
|---|---|---|---|---|---|---|---|
| May 25, 1987 | 0859:12.46 | 63°54.31′ | 19°45.68′ | 9.9 | 3.8 | 0.5 | 1.3 |
| May 25, 1987 | 0859:40.44 | 63°54.89′ | 19°46.27′ | 10.6 | 3.0 | 0.8 | 1.5 |
| May 25, 1987 | 0900:35.93 | 63°55.07′ | 19°46.41′ | 7.9 | 2.8 | 0.6 | 2.8 |
| May 25, 1987 | 0901:24.26 | 63°54.55′ | 19°45.64′ | 10.4 | 2.8 | 0.4 | 1.1 |
| May 25, 1987 | 1025:38.36 | 63°55.67′ | 19°46.22′ | 11.8 | 2.0 | 0.5 | 0.9 |
| May 25, 1987 | 1050:26.13 | 63°55.23′ | 19°47.84′ | 12.1 | 1.6 | 0.6 | 1.1 |
| May 25, 1987 | 1130:07.36 | 63°55.28′ | 19°46.08′ | 12.2 | 1.8 | 0.6 | 1.0 |
| May 25, 1987 | 1131:54.70 | 63°54.54′ | 19°46.75′ | 11.3 | 5.5 | 0.6 | 1.3 |
| May 25, 1987 | 1135:38.28 | 63°56.45′ | 19°47.09′ | 7.3 | 3.5 | 0.4 | 0.9 |
| May 25, 1987 | 1138:37.54 | 63°52.60′ | 19°44.42′ | 12.1 | 3.2 | 0.5 | 1.4 |
| May 25, 1987 | 1143:38.49 | 63°54.32′ | 19°45.39′ | 6.9 | 2.7 | 0.4 | 2.3 |
| May 25, 1987 | 1147:14.95 | 63°53.28′ | 19°46.09′ | 11.7 | 2.0 | 0.6 | 1.4 |
| May 25, 1987 | 1148:15.99 | 63°53.37′ | 19°46.45′ | 10.7 | 3.3 | 0.5 | 1.5 |
| May 25, 1987 | 1149:11.90 | 63°51.48′ | 19°46.79′ | 10.5 | 2.4 | 1.8 | 3.3 |
| May 25, 1987 | 1154:57.52 | 63°53.09′ | 19°44.41′ | 11.1 | 2.4 | 0.6 | 1.6 |
| May 25, 1987 | 1155:42.38 | 63°53.19′ | 19°44.62′ | 8.4 | 1.8 | 0.7 | 1.6 |
| May 25, 1987 | 1156:06.41 | 63°53.86′ | 19°44.99′ | 6.1 | 2.2 | 0.6 | 2.7 |
| May 25, 1987 | 1159:53.48 | 63°53.85′ | 19°44.75′ | 8.6 | 2.5 | 0.4 | 1.1 |
| May 25, 1987 | 1206:03.08 | 63°53.05′ | 19°46.71′ | 8.3 | 2.0 | 0.4 | 1.2 |
| May 25, 1987 | 1213:02.41 | 63°51.85′ | 19°49.74′ | 13.1 | 2.2 | 0.5 | 1.2 |
| May 25, 1987 | 1213:27.64 | 63°53.17′ | 19°45.36′ | 6.1 | 2.8 | 0.4 | 1.4 |
| May 25, 1987 | 1221:50.49 | 63°53.79′ | 19°45.88′ | 8.2 | 3.6 | 0.6 | 1.8 |
| May 25, 1987 | 1225:58.91 | 63°55.38′ | 19°46.23′ | 10.7 | 2.2 | 0.4 | 1.1 |
| May 25, 1987 | 1234:23.47 | 63°55.04′ | 19°45.76′ | 11.2 | 1.7 | 0.6 | 1.3 |
| May 25, 1987 | 1243:26.47 | 63°52.94′ | 19°47.51′ | 10.5 | 2.0 | 0.6 | 1.5 |
| May 25, 1987 | 1342:40.49 | 63°54.58′ | 19°44.21′ | 7.1 | 2.8 | 0.4 | 1.2 |
| May 25, 1987 | 1343:46.28 | 63°54.64′ | 19°44.15′ | 7.6 | 2.3 | 0.7 | 2.1 |
| May 25, 1987 | 1344:10.35 | 63°56.19′ | 19°42.72′ | 11.2 | 2.4 | 0.5 | 1.1 |
| May 25, 1987 | 1405:03.36 | 63°52.53′ | 19°47.77′ | 11.5 | 2.1 | 0.5 | 1.3 |
| May 25, 1987 | 1416:25.28 | 63°55.45′ | 19°43.44′ | 8.6 | 2.3 | 0.6 | 1.4 |
| May 25, 1987 | 1431:49.00 | 63°52.82′ | 19°47.17′ | 12.8 | 1.9 | 0.5 | 1.2 |
| May 25, 1987 | 1933:01.85 | 63°52.46′ | 19°45.82′ | 7.5 | 2.1 | 0.4 | 1.3 |
| May 25, 1987 | 2145:25.85 | 63°53.90′ | 19°44.46′ | 7.7 | 3.0 | 0.6 | 1.8 |
| May 25, 1987 | 2201:00.55 | 63°54.55′ | 19°43.23′ | 7.6 | 1.8 | 0.6 | 1.5 |
| May 26, 1987 | 0030:15.97 | 63°55.05′ | 19°46.50′ | 11.5 | 2.0 | 0.8 | 1.4 |
| May 26, 1987 | 0920:59.96 | 63°54.38′ | 19°44.33′ | 10.2 | 3.2 | 0.5 | 1.4 |
| May 27, 1987 | 0256:33.44 | 63°53.47′ | 19°43.48′ | 7.5 | 2.3 | 0.5 | 1.7 |
| May 27, 1987 | 0603:54.33 | 63°57.80′ | 19°45.08′ | 6.1 | 2.3 | 0.5 | 0.8 |
| June 02, 1987 | 1652:15.14 | 63°53.63′ | 19°44.59′ | 4.8 | 2.1 | 0.5 | 1.3 |
| June 29, 1987 | 0201:36.50 | 63°56.75′ | 19°44.60′ | 9.3 | 2.5 | 0.4 | 0.8 |

The magnitudes are based on the duration of the seismic signal on local seismograms.
[a]Uncertainty in the horizontal and vertical location at one standard error [*Klein*, 1978].

shocks of magnitude less than three were recorded in June, but since then the area has been relatively quiet.

The earthquake sequence was recorded on the local network of short period seismographs, which is relatively dense in this region (Figure 1). Fifteen instruments were in operation within a 100-km distance, and the nearest station was generally within 15 km of the events. The location program HYPOINVERSE by *Klein* [1978] was used, with a crustal model based on the RRISP 77 deep refraction profile [*Angenheister et al.*, 1980; *Gebrande et al.*, 1980] that was run close to this area. The model is one-dimensional, and consists of several layers with constant velocity gradients but no discontinuites in velocity (Table 2). Station corrections have been found by trial and error in locating earthquakes and explosions of known origin. Six to seventeen readings were used in the location of the earthquake sequence, and the RMS time differences were generally less than 0.15 s. Absolute locations found by this method are generally accurate within 1 km, and the calculated standard error (see Table 1) can be regarded as a resonable representation of relative location error.

The epicentral area of the earthquakes is at the western foot of the main Vatnafjöll edifice (Figures 3 and 4). It is elongate in the N-S direction, about 12 km long and 4 km wide. Hypocentral depths of almost all events are in the range 6–13 km (Figure 5). The earthquakes thus occurred in the lower part of the crust, which extends to 14 km depth in this area. The mainshock hypocenter is located at 11 km depth. The foreshocks all occurred within a 2 km horizontal distance of the mainshock (Figure 3). They by themselves define a narrow, N-S trending zone, which is 3 km long. The first few locatable aftershocks extend over a narrow 8 km long zone, and 17 min after the mainshock the aftershocks extend over 10-km-long zone. The two northernmost shocks occurred on May 27 and June 29, after the main activity was over. We conclude from the hypocentral distribution and the time sequence of the events, that the lower part of the crust was ruptured along a N-S striking fault. The rupture extended 10 km and possibly as much as 12 km along the fault.

The 4-km width of the epicentral zone is larger than can be accounted for by the horizontal errors of the locations (Table 1). More than one fault seems to be involved. The zone is narrow in the middle and broadens out toward the ends. If one plots only the foreshocks and the aftershocks of the first half hour, 18 events in all, a much narrower zone emerges (Figure 4). This zone is about 1.5 km wide and has a strike of 345°. Aftershocks in the following 21 hours define a second zone, similarly narrow, with a strike of about 35°. The significance of this observation is not clear at this time.

TABLE 2. Crustal Structure

| Depth km | $V_P$, km/s | $V_S$, km/s | Density, g/cm$^3$ |
|---|---|---|---|
| | *Local Model*[a] | | |
| 0.0 | 3.40 | 1.96 | |
| 1.5 | 4.60 | 2.66 | |
| 9.0 | 6.50 | 3.75 | |
| 14.0 | 7.00 | 4.04 | |
| 32.0 | 7.40 | 4.27 | |
| | *Source Model*[b] | | |
| 0.0 | 4.00 | 2.31 | 2.30 |
| 1.5 | 5.55 | 3.20 | 2.75 |
| 9.0 | 6.75 | 3.90 | 3.00 |
| 14.0 | 7.20 | 4.16 | 3.10 |
| | *Receiver Model*[b] | | |
| 0.0 | 6.00 | 3.46 | 2.75 |

[a]Used in location of earthquake sequence. Layers have constant velocity gradients.

[b]Used in calculation of synthetic seismograms. Layers have constant velocities.

## Surface Effects

As soon as the epicentral area had been determined with sufficient accuracy, a reconnaissance party went to the area to study possible surface effects or faulting. Abundant evidence of heavy shaking were found, such as rock falls, overturned rocks and gravel, soil cracks, and snow avalanches [*Einarsson*, 1988]. No evidence of bedrock faulting at the surface could be found, in spite of considerable search. Soil cracks that were found were randomly oriented and had no resemblance to the regular faulting pattern described by *Einarsson and Eiríksson* [1982] from other parts of the seismic zone. It is concluded that crustal faulting did not extend to the surface in this earthquake.

## Waveform Inversion

We determined the best fitting double-couple point source from inversion of long-period (vertical component) $P$ and long-period $SH$ waveforms using the inversion technique of *Nábělek* [1984, 1985]. Parameters estimated by the inversion are the double-couple orientation, centroid depth, seismic moment, and apparent source time function. The seismograms used were recorded by Canadian, Global Digital Seismic Network (GDSN) and World-Wide Standard Seismograph Network (WWSSN) stations at epicentral distances between 30° and 90° for $P$ waves and 30° and 70° for $SH$ waves (Table 3). In these distance ranges the travel time curves do not have multiplications, which makes it simple to calculate the Greens functions. Seismograms recorded by Canadian and WWSSN stations were hand digitized and interpolated at intervals of 0.5 s. Amplitudes were equalized to an instrument magnification of 1500 at a distance of 40°. For the inversion we used a layered velocity model for the source region based on the same gradient velocity model that was used above for locating the earthquake sequence. The density profile in the source region is based on a compilation by *Ryan* [1987] (Table 2). The receiver crustal structure (Table 2) is expected to be adequately approximated by a half-space [*Nábělek*, 1984]. To account for anelastic attenuation, we used the conventional $t*$ values of 1.0 and 4.0 s for long-period $P$ and $SH$ waves respectively [*Futterman*, 1962]. The far-field source time function is parameterized by a series of overlapping isosceles triangles of preassigned number and duration. The relative amplitudes of the triangles are determined by the inversion.

The estimated values of the parameters of the best fitting double-couple point source are those which minimize the mean square residual $R^2$ defined as

$$R^2 = \frac{\sum_{j=1}^{N} \sum_{i=1}^{M_j} {w_j}^2 (s_{ij} - o_{ij})^2}{\sum_{j=1}^{N} M_j} \qquad (1)$$

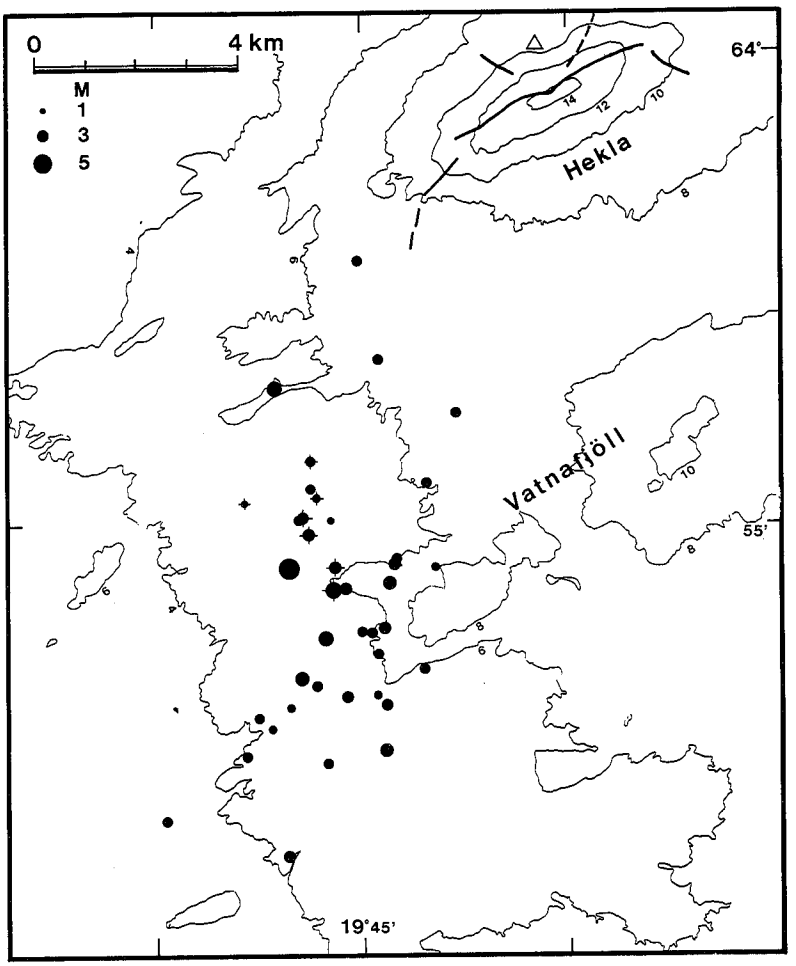


Fig. 3. Epicenters of the Vatnafjöll sequence. Foreshocks are marked with a cross. Elevation is contoured at 200-m intervals. The nearest seismograph, marked with a triangle, is north of the summit of Hekla, on the 1000-m contour. The eruptive fissures active in the Hekla eruptions of 1980–81 are shown with thick solid lines [*Grönvold et al.*, 1983]. The epicentral zone is elongate in the N-S direction and bridges the gap between the Vatnafjöll and Hekla volcanic systems.

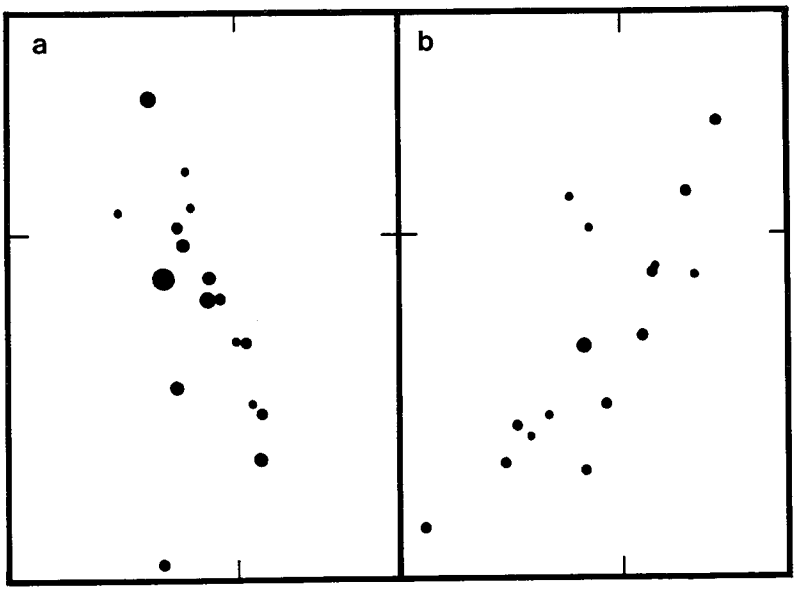


Fig. 4. (*a*) Epicenters before 1210 UT, and (*b*) epicenters of the following 12 hours.

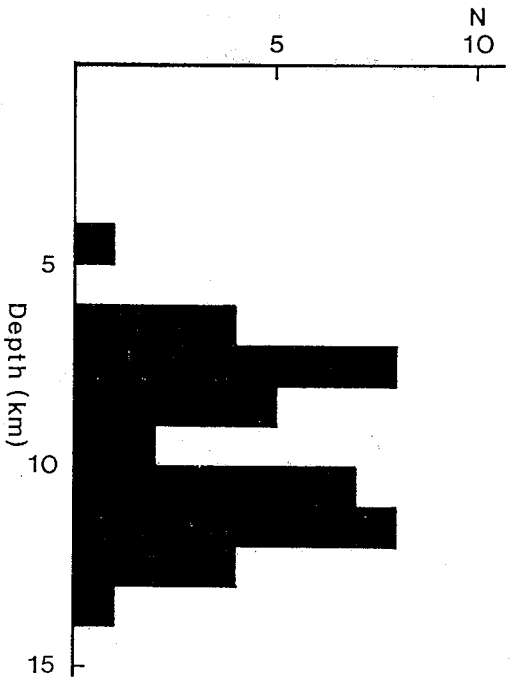


Fig. 5. Histogram of hypocentral depths of the Vatnafjöll sequence. $N$ is the number of events within the respective 1-km depth interval.

where $s_{ij}$ and $o_{ij}$ are the amplitudes of the $j$th synthetic and observed seismograms at time sample $i$, $w_j$ is the weight used for the $j$th seismogram, $M_j$ is the number of samples in the time window used in the inversion for seismogram $j$, and $N$ is the total number of $P$ and $SH$ seismograms used in the inversion. Because of the larger amplitudes of the $SH$ waves relative to the $P$ waves, the weights of the $SH$ seismograms were decreased in order to give $P$ and $SH$ waves equal weight in the inversion. In addition, weights were applied to compensate for uneven azimuthal coverage of stations (Table 3). The station weights, $w_j$, are proportional to $1/\sqrt{n+1}$, where $n$ is the number of stations within $\pm 15°$ of azimuth from the $j'th$ station on the $P$ and $SH$ focal planes, respectively. This weighting scheme attempts to obtain equitable weighting of the stations in a least squares sense.

As a starting model for the inversion, we give the source time function an overestimated duration with all triangular elements of equal amplitude. After several inversion experiments it was found that the source time function elements beyond 3 s had zero or near-zero amplitude. They were therefore discarded in subsequent inversions. Between the inversions we realign the synthetic and observed seismograms in order to get the best correlation between them and in turn to minimize $R^2$. When the point source is positioned at the fault centroid the best overall correlation between the observed and synthetic seismograms is obtained

TABLE 3. Station Parameters Used in Body Wave Inversion

| Station | Azimuth, deg | Distance, deg | Weights $P/SH$ | Wave, Used |
|---|---|---|---|---|
| MAJO | 17.9 | 78.2 | 0.00 | SH* |
| BJI | 34.9 | 70.7 | 0.71/0.21 | P/SH |
| TATO | 34.6 | 86.2 | 0.71/0.00 | P/SH* |
| KMI | 54.1 | 80.6 | 0.00 | SH* |
| CHTO | 56.3 | 85.0 | 1.00/0.00 | P/SH* |
| ANTO | 102.6 | 38.7 | 0.71/0.11 | P/SH* |
| IST | 105.4 | 36.1 | 0.11 | SH |
| HLW | 111.7 | 46.7 | 0.58/0.11 | P/SH |
| AAE | 114.9 | 68.4 | 0.11 | SH |
| AQU | 122.6 | 28.8 | 0.58/0.11 | P/SH |
| BCAO | 137.1 | 65.6 | 0.71/0.15 | P/SH |
| BDF | 207.3 | 82.3 | 0.00 | SH* |
| ZOBO | 226.0 | 88.2 | 0.71 | P |
| BOG | 239.1 | 70.8 | 0.71 | P |
| WES | 258.7 | 36.2 | 0.58 | P |
| SHA | 265.8 | 53.3 | 0.15 | SH |
| OTT | 266.1 | 35.7 | 0.58 | P |
| GAC | 266.2 | 35.4 | 0.58/0.15 | P/SH |
| ALQ | 284.4 | 57.7 | 0.58 | P |
| ANMO | 284.4 | 57.7 | 0.15 | SH |
| FFC | 296.4 | 39.7 | 0.45 | P |
| CMBD | 297.4 | 60.8 | 0.45/0.11 | P/SH |
| EDM | 302.9 | 45.5 | 0.45 | P |
| LOND | 303.8 | 53.9 | 0.45/0.12 | P/SH |
| PNT | 304.0 | 50.9 | 0.12 | SH |
| YKC | 314.1 | 38.0 | 0.50 | P |
| INK | 328.0 | 39.9 | 0.50/0.21 | P/SH |
| COLD | 332.2 | 45.8 | 0.58 | P |
| MBC | 333.1 | 31.4 | 0.58 | P |

*The $SH$ waveform was not used in the inversion, but the corresponding synthetic seismogram was calculated.

[*Dziewonski et al.*, 1981; *Nábělek*, 1984]. However, at the best overall correlation between the observed and synthetic seismograms, the first motion of the synthetic seismogram does not necessarily align with the observed first motion.

From the inversion of $P$ and $SH$ waveforms of the Vatnafjöll earthquake we obtain for the best fitting double-couple point source a nearly pure strike slip focal mechanism $6° \pm 5°/93° \pm 5°/185° \pm 5°$ (strike/dip/rake) (Figure 6), with seismic moment $9.1 \pm 1.7 \times 10^{24}$ dyn cm and centroid depth of $6.6 \pm 1.6$ km (Table 4). The uncertainties are within two standard deviations for the seismic moment and centroid depth and within 10 standard deviations for the focal mechanism parameters. The uncertainties in focal mechanism parameters and seismic moment are obtained directly from the inversion, but the uncertainty in centroid depth is from a statistical $t$ test which is described below. Error analyses have shown that 10 standard deviations are more representative of uncertainty in the focal mechanism parameters [*Nábělek*, 1984]. The centroid depth is given relative to the top of the crust and we follow *Aki and Richards* [1980] in describing the double couple orientation. The waveforms generally fit very well. Some of the $SH$ waveforms, labeled by asterisks in Figure 6, were not used in the inversion because they were recorded by stations at distances greater than 70° from the source. However the calculated synthetic seismograms from the best double-couple point source fit most of these stations very well and the first motion is the same as the observed. At these distances, 70°–90°, the $ScS$ arrives 20–40 s after the $S$ and has the same polarity. Therefore the agreement between the synthetic and observed first motion of these stations is a significant observation. The best fitting focal mechanism from the inversion agrees perfectly with $P$ wave first motion of all available long-period (vertical) seismograms (Figure 7).

## Statistics And Error Analysis

The centroid depth is an important parameter for interpretation of the rupture. It is therefore essential to know the resolution of the estimated centroid depth determined by the inversion. Depending on the data the estimated centroid depth can be quite nonunique and have little statistical significance [*Huang*, 1985; *Huang et al.*, 1986].

We performed a statistical test to estimate the resolution of centroid depth. This was done by testing the significance of difference in waveform fit between the overall best solution against a range of solutions which were found by fixing the centroid depth while inverting for the remaining source parameters. In the search for the best solution at a fixed depth, we followed the same procedures as before when determining the overall best solution, by varying the source time function length and realigning the synthetic and observed seismograms to improve the fit.

The variance versus depth curve (Figure 8*a*) shows a clear global minimum at the optimal centroid depth. The local minimum at 9 km is probably caused by a layer boundary in the source velocity model [*Huang*, 1985]. We followed *Huang et al.* [1986] in estimating the uncertainty in the centroid depth by using paired $t$ test of significance for the differences between the residuals of each synthetic and observed seismogram pair at the optimal centroid depth and at a range of fixed depths. The mean squared residual for seismogram $j$ is defined as

$$r_j = \frac{1}{M_j} \sum_{i=1}^{M_j} w_j{}^2 (o_{ij} - s_{ij})^2 \qquad (2)$$

and the set of seismogram residual differences (the statistical samples) at depth $k$ and the optimal depth $o$ is defined as

$$d_j = r_{jk}^2 - r_{jo}^2 \qquad j = 1, 2, \cdots, N \qquad (3)$$

where $N$ is the number of seismograms used in the inversion. The $t$ test of significance assumes normally distributed samples. The $\chi^2$ test for goodness of fit showed that our sets of $d_j$ are normally distributed and we denote the mean and standard deviation of the set $d_j$ with $\mu_d$ and $\sigma_d$, respectively. We tested the null hypothesis $\mu_d = 0$ against the alternative one-sided hypothesis $\mu_d > 0$. The test statistic is

$$t = \frac{\mu_d \sqrt{N}}{\sigma_d} \qquad (4)$$

which follows the $t$ distribution with $N$-1 degrees of freedom.

Figure 8*b* shows the $t$ statistic at the 0.05 significance level as a horizontal straight line. This statistic is exceeded at depths greater than 5.0 km and less than 8.0 km. Hence we can say with 95% confidence that the best fitting centroid depth lies between 5.0 and 8.0 km depth. On the basis of this test we conclude that the estimated centroid depth of 6.6 km is well constrained. In fact, the centroid depth is unusually well constrained for a waveform inversion of long period data. We think the reason for this might be due to relatively high-frequency content of the many Canadian waveforms that were used in this study.

The other source parameters from the inversion can also be regarded as well constrained. Although we did not test statistically the significance of them, it is possible to draw inferences on the stability of these parameters with depth, using the results from the test of significance of the centroid depth. That test showed that the focal mechanism is very stable with depth. In the centroid depth range of 4.0–12.0 km the angular parameters are within ±5° of the best solution and within ±1° in the 95% confidence range of the centroid depth. The source time function has constant duration within the 95% confidence range of the centroid depth. It has, however, both emergent and impulsive shape within this depth range. For this reason we do not believe that the shape of the source time function has any significance, based on the current long period data set.

## Discussion

Two types of evidence show that the Vatnafjöll earthquake should be classified as a transform event rather than a rift zone event. First of all, the focal mechanism is strike slip on a northerly striking fault, which is the same type of faulting as inferred from surface fractures in the South Iceland Seismic Zone farther west [*Einarsson and Eiríksson*, 1982]. Fault plane solutions along divergent parts of the Mid-Atlantic plate boundary usually show dip slip faulting [*Einarsson*, 1986]. Second, the relatively large magnitude of the event is not typical for rift zone events in Iceland.

The eastern part of the South Iceland Seismic Zone has been rather quiet seismically in the last decades. It has therefore been difficult to determine how far the zone extends toward the east. The best evidence so far has been the area of destruction associated with the 1912 earthquake,

# P WAVES

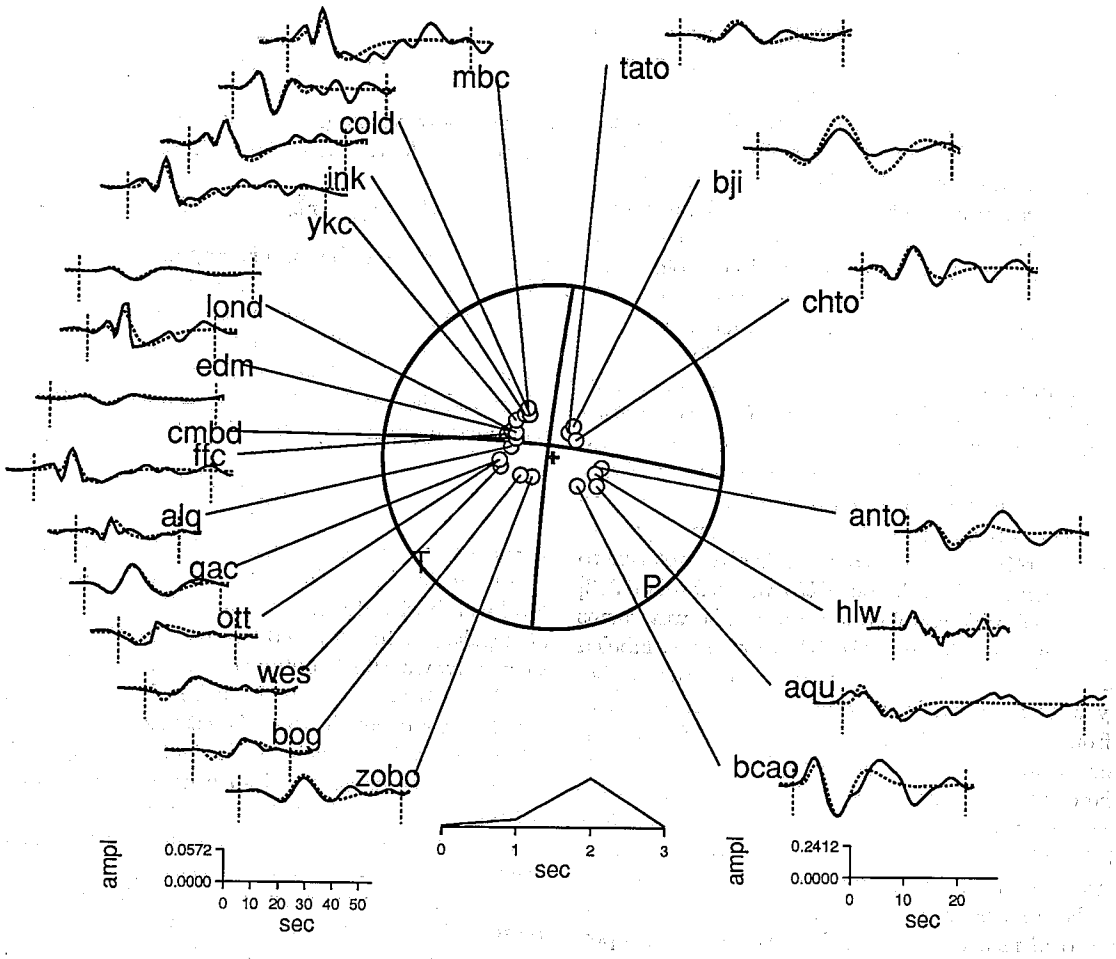


# SH WAVES

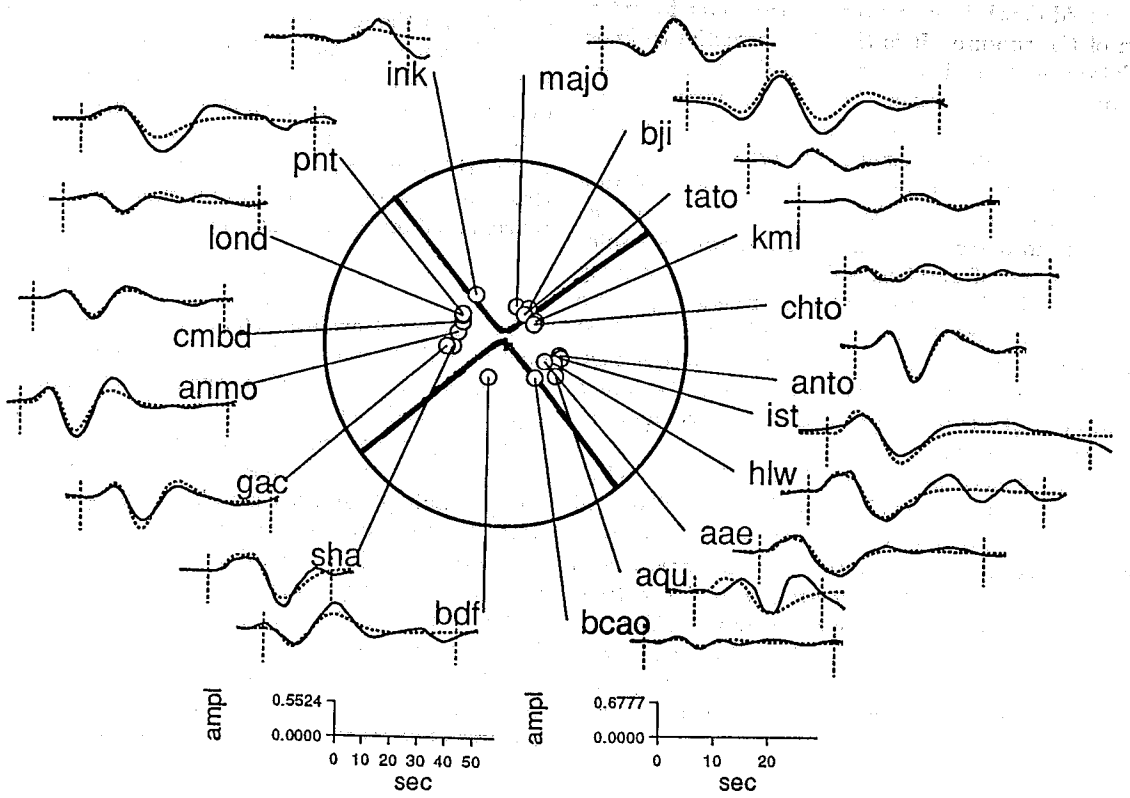

TABLE 4. Source Parameters of Vatnafjöll Earthquake

| Parameter | Value |
|---|---|
| Origin time[a] | May 25, 1987, 1131:54.7 UT |
| Magnitude[b] | 5.8 ($m_b$), 5.8 ($M_S$), 5.9 ($M_w$) |
| Epicenter[a] | 63.91°N, 19.78°W |
| Hypocenter Depth[a] | $11 \pm 3$ km |
| Centroid Depth[c] | $6.6 \pm 1.6$ km |
| Mechanism[d,e] (strike/dip/rake) | $6° \pm 5°/ 93° \pm 5°/ 185° \pm 5°$ |
| Moment[f] | $9.1 \pm 1.7 \times 10^{24}$ dyn cm |
| Source Duration[f], | $3 \pm 1$ s |

[a]Hypocenter parameters determined with local data, uncertainty in hypocenter depth at two standard deviations (2.4 x standard error) [*Klein*, 1978].

[b] $M_S$ and $m_b$ magnitudes are from EDR.

[c]Centroid depth relative to top of crust, uncertainty within the 95% confidence level is determined by statistical $t$ test.

[d]Focal mechanism specified with convention of *Aki and Richards* [1980].

[e]Uncertainty at 10 standard deviations is determined directly from inversion.

[f]Uncertainty at 2 standard deviations is determined directly from inversion.

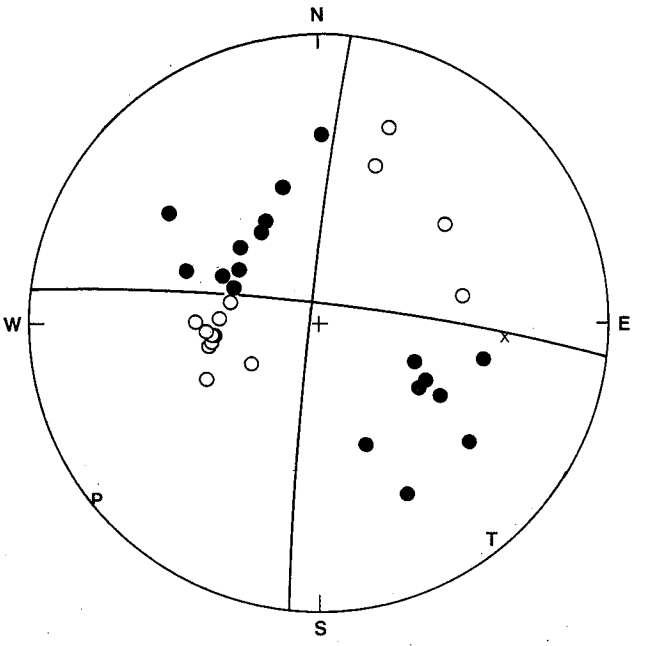


Fig. 7. $P$ wave first motions plotted on equal-area lower hemisphere diagram. Solid circles represent compressions and open circles dilatations. Nodal motions are marked with a cross. $P$ and $T$ axes are shown.

but since the area east of it has been unpopulated, it is not known if historical events occurred farther east. The 1987 event shows that the seismic zone extends at least to Vatnafjöll and perhaps as far as the Torfajökull central volcano in the middle of the rift zone (Figure 1). The transform zone is therefore some 30 km longer than has been known with certainty before.

The magnitude of the Vatnafjöll earthquake is 5.8, measured both from body waves ($m_b$) and surface waves ($M_S$), and it has a moment magnitude $M_w$ of 5.9.

We made estimates of the fault dimensions, average stress drop and slip for the Vatnafjöll earthquake, based on the information on the distribution of aftershocks and seismic moment. We assume a circular fault model with source radius, $r$, of $5 \pm 2$ km inferred from the distribution of aftershocks. An average stress drop, $\Delta\sigma$, of $32 \pm 39$ bars was estimated from the relation $\Delta\sigma = \frac{7}{16} Mo/r^3$ [*Eshelby*, 1957; *Kanamori and Anderson*, 1975]. An average slip of $32 \pm 27$ cm was estimated from the relation $M_o = \mu \Delta u S$ [*Aki*, 1966], where $\Delta u$ is the average slip, $S$ is the fault area and average rigidity, $\mu$ of the source region was calculated from the source crustal structure to be $3.6 \times 10^{11}$dyn/cm$^2$. The uncertainties can be regarded to be related to two standard deviations. The large uncertainties in these calculations make it impossible to assert anything about the stress drop of this earthquake. Other factors, however, indicate that the Vatnafjöll earthquake had higher than average stress drop. Many of the $P$ wave waveforms have relatively high-frequency content, indicating high stress drop. The source time function of this earthquake has about 1/3 shorter duration than the global average of earthquakes of this size [*Ekström and Engdahl*, 1989], also indicating higher than average stress drop.

The hypocentral and centroid depths of the earthquake show that the rupture was initiated near the base of the crust and then propagated mainly upward. It did not reach the surface, which is confirmed by the absence of surface ruptures. The centroid depth is shallower than the geometric center of the aftershock area. Assuming that the aftershock area is within the source radius, it suggests that slip decreased with depth. It could also mean that larger proportion of the fault area is in the upper crust, than is indicated by the aftershock area.

The Vatnafjöll earthquake has some important implications for previous estimates of the magnitudes of past earthquakes in the seismic zone, which are important for the assessment of seismic risk in the populated parts of the zone. The 1912 earthquake is the only large event so far with an instrumentally determined magnitude $M_S = 7$ [*Kárnik*, 1969]. Magnitudes of other events have been estimated by comparing their destruction areas with that of the 1912 event [*Halldórsson et al.*, 1984]. Magnitudes between 6.7 and 7.1

Fig. 6. Observed long-period (vertical) $P$ and $SH$ waves (solid lines) and synthetic waveforms (dashed lines) as predicted by the best fitting double-couple point source obtained by the body wave inversion. Waveforms are shown on lower focal hemisphere equal-area projection. $P$ and $T$ axes are shown, and $SH$ positive motion is as defined by *Aki and Richards* [1980]. Amplitudes were normalized to an instrument magnification of 1500 at distance of 40°. The amplitude scales, shown at the bottom of the figures, correspond to waveform amplitudes in centimeters that would be observed on an original seismogram for such an instrument. The scales to the left are for Canadian and WWSSN seismograms and the scales to the right are for GDSN seismograms. $SH$ waves labelled with asterisks were not used in the inversion. The parts of the seismograms that were used in the inversion are delimited with two vertical bars. The first bar represents the arrival of the synthetic first motion.

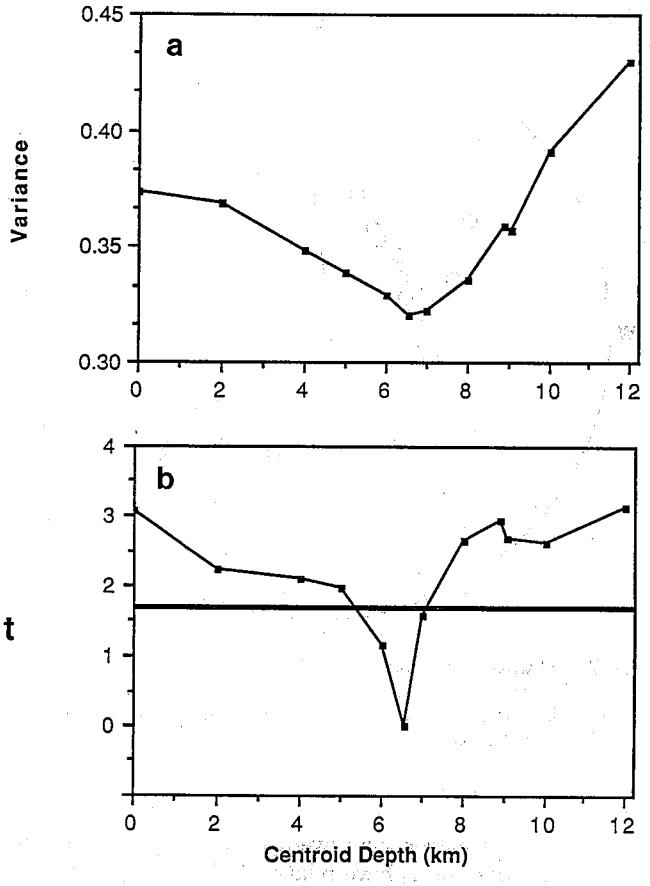


Fig. 8. (a) Variance of misfit (normalized by power of seismograms) of a best fit double-couple point source at a range of centroid depths. (b) $t$ statistic versus centroid depth. The horizontal line is the 0.05 significance level. Hence the 95% confidence interval for the best fitting centroid depth lies within 5.0-8.0 km depth

have been obtained for the largest events since 1700. These maximum magnitudes are comparable to those of earthquakes along other Atlantic transform faults. An interesting problem arises, however, because of the peculiar circumstances in the South Iceland Seismic Zone. The faults are perpendicular to the zone, and the width of the seismic zone is only 10–15 km as determined from microearthquake distribution and mapped surface fractures. The length of each fault therefore has an upper limit of about 15 km. Using this maximum fault length and assuming that the whole crust is ruptured down to 14 km one can attempt to estimate the slip required to produce an earthquake of magnitude 7. For this estimation we use two different methods. The first method uses the Gutenberg-Richter empirical relation between seismic energy and surface wave magnitude. The second method uses the *Hanks and Kanamori* [1979] moment-magnitude relation.

The Gutenberg-Richter empirical energy relation is given by

$$\log E_s = 1.5M_s + 11.8 \tag{5}$$

where the seismic energy $E_s$ is measured in ergs. Combining (5) with $E_s = \frac{\Delta\sigma}{2\mu} M_o$ , $\Delta\sigma = c\mu\frac{\Delta u}{w}$, and $M_o = \mu\Delta u L w$, gives

$$\Delta u = \sqrt{\frac{2E_s}{c\mu L}} \tag{6}$$

where $\Delta u$ is average slip, $L$, $w$ are length and width of the fault plane, and c is a geometric constant which is approximately unity. Equivalent relation to (6) for a circular fault model is

$$\Delta u = \sqrt{\frac{2E_s}{c\mu\pi r}} \tag{7}$$

where $r$ is the fault radius and the geometric constant is $c = \frac{7\pi}{16}$ . Applying (5) and (7) to the Vatnafjöll earthquake gives an average slip of 29 cm, which agrees very well with the previous estimate of 32 cm. Similarly, for a magnitude 7.0 earthquake in the South Iceland Seismic Zone an average slip of 2.7 m can be calculated by using equations (5) and (6) with source parameters as described above. This is a large slip for only 15-km-long faults, however it seems to be a reasonable estimate based on available field observations. The only direct field measurement of fault slip is 0.7–0.8 m near the southern end of the 1896 surface rupture in the Land district [*Einarsson and Eiríksson*, 1982]. The measurement is taken at a displaced wall built of turf and stones. As this measurement is near the terminus of the fault we think it is not inconsistent with our determined estimate of average slip for a magnitude 7 earthquake in south Iceland.

The faults in the South Iceland Seismic Zone are generally characterized by en echelon tension gashes separated by compressional pushups. Historic and field evidence indicate that most of the surface fractures resulted from single strike-slip earthquakes [*Einarsson and Eiríksson*, 1982]. Some of the pushups seem to be created by a simple buckling of the surface lava flows. In these cases the slip of the underlying fault can be estimated to be approximately equal to the shortening of the surface lava flow. The pushups are up to 3–4 m high and 12–15 m in diameter. The shortening can be calculated with $d(\frac{1}{\cos\phi} - 1)$, where $d$ is the diameter and $\phi$ is the slope of the pushup. This gives an approximate estimate of slip up to 2.5 m. Again, we think that this supports our notion of unusually large ratio of slip to fault length for large south Iceland earthquakes.

*Scholz et al.* [1986] determined a scaling law between fault slip and fault length of large earthquakes and observed that intraplate earthquakes have on average 6 times greater slip than interplate earthquakes of same fault length. A 2.7-m slip on a 15-km-long fault is, however, about 18 times the average proportional slip of interplate earthquakes or 3 times the average proportional slip of intraplate earthquakes. The stress drop corresponding to the 2.7 m slip is 70 bars. This is relatively high stress drop and is in the range of stress drops of intraplate earthquakes [*Kanamori and Anderson*, 1975].

The second method to estimate average slip and stress drop assumes that the *Hanks and Kanamori* [1979] moment magnitude relation $M_w = \frac{2}{3}\log M_\phi - 10.7$ applies to earthquakes in south Iceland of magnitude 7. Combined with $M_o = \mu\Delta u L w$ and $\Delta\sigma = c\mu\frac{\Delta u}{w}$, this method gives even higher estimates, 5.3 m average slip and 135 bars stress drop.

On the basis of either of the two stress drop estimates above, the faults of the South Iceland Seismic Zone can be termed as strong faults. Stress drop is a parameter that scales proportionally to maximum acceleration [*Brune*, 1970]. However, at this stage we can not predict the maxi-

mum acceleration of a magnitude 7 earthquake in the South Iceland Seismic Zone, because it depends on some other factors that are not the subject of this paper.

The South Iceland Seismic Zone is clearly a plate boundary related region, but the estimated large slip and high stress drop of earthquakes in this region are more in common with intraplate earthquakes. The distinction between interplate and intraplate earthquakes is based on the slip rate of their faults and their recurrence time [*Scholz et al.*, 1986; *Kanamori and Allen*, 1986]. A recent study on structural evolution of strike-slip faults found that the number of steps in a fault trace per unit length decrease with increasing total slip of the faults [*Wesnousky*, 1988]. Earthquake rupture often terminates at steps in the fault trace, and hence they are thought to be the strong parts of the fault. These observations tend to support the hypothesis of *Scholz et el.* [1986] that the difference in total slip between intraplate faults and interplate faults may play a role in the greater strength of intraplate faults. The South Iceland Seismic Zone faults are young and have therefore accumulated small total slip. We do not at present have reliable information on the slip rate and recurrence time of individual faults in the South Iceland Seismic Zone. With that information in hand, these faults could supply decisive data on wether recurrence time or total slip is the more important variable that governs strength of faults.

## CONCLUSIONS

1. The 1987 Vatnafjöll earthquake occurred in the Eastern Volcanic Zone, but in a direct continuation of the South Iceland Seismic Zone, where it extends into the volcanic zone.

2. The earthquake was associated with right-lateral strike-slip faulting on a nearly vertical fault with a northerly strike. It therefore resembles earthquakes in the South Iceland Seismic Zone to the west and is probably not related to magmatic activity in the Vatnafjöll volcanic system. The transform zone is thus shown to extend farther into the rift zone than was previously recognized, perhaps all the way to the Torfajökull central volcano.

3. Based on the distribution of foreshocks and aftershocks, it appears that the rupture was initiated near the base of the crust and propagated bilaterally and upwards. It did not reach the surface, however. This shows that larger earthquakes can occur in this part of the seismic zone, well within the Eastern Volcanic Zone.

TABLE 5. Source Parameters

| Parameter | Value |
|---|---|
| Seismic moment | $9.1 \pm 1.7 \times 10^{24}$ dyn cm |
| Mechanism (strike/slip/rake) | $6° \pm 5°/93° \pm 5°/185° \pm 5°$ |
| Source duration | $3 \pm 1$ s |
| Centroid depth | $6.6 \pm 1.6$ km |
| Hypocentral depth | $11 \pm 3$ km |
| Source radius | $5 \pm 2$ km |
| Average stress drop | $32 \pm 39$ bars |
| Average displacement | $32 \pm 27$ cm |

Uncertainties are at or within two standard deviations, except for the focal mechanism parameters, where uncertainties are given with the more appropriate 10 standard deviations.

4. The values in Table 5 were obtained for the source parameters.

*Acknowledgments.* We thank William Menke, Paul Huang, Göran Ekström, Christopher Scholz, and Arthur Lerner-Lam for useful discussions and comments that improved this work. John Nábělek kindly allowed the use of his waveform inversion program and gave good advice on how to digitize seismograms. Operators of the Albuquerque Seismological Laboratory, the Canadian, and the WWSSN networks generously supplied seismic records for this work. This research was supported by the NSF under grant EAR87-96171. Partial support also came from a NATO Science fellowship. LDGO contribution 4735.

## REFERENCES

Aki, K., Generation and propagation of *G* waves from the Niigata earthquake of June 16, 1964, 2, Estimation of earthquake moment, released energy, and stress-strain drop from the *G* wave spectrum, *Bull. Earthquake Res. Inst. Univ. Tokyo, 44,* 73–88, 1966.

Aki, K., and P. G. Richards, *Quantitative Seismology: Theory and Methods,* vol. 1, W. H. Freeman, New York, 1980.

Angenheister, G., et al., Reykjanes Ridge Iceland Seismic Experiment (RRISP 77), *J. Geophys., 47,* 228–238, 1980.

Brune, J. N., Tectonic stress and spectra of seismic shear waves from earthquakes, *J. Geophys. Res., 75,* 4997–5009, 1970.

Dziewonski, A. M., T. A. Chou, and J. H. Woodhouse, Determination of earthquake source parameters from waveform data for studies of global and regional seismicity, *J. Geophys. Res., 86,* 2825–2852, 1981.

Einarsson, P., Jardskjálftaspár, (in Icelandic with an English abstract), *Náttúrufræðingurinn, 55,* 9–28, 1985.

Einarsson, P., Seismicity along the eastern margin of the North American Plate, in *The Geology of North America,* vol. M, *The Western North Atlantic Region,* edited by P. R. Vogt, and B. E. Tucholke , pp. 99–116, Geological Society of America, Boulder, Colo., 1986.

Einarsson, P., The earthquake in Vatnafjöll, May 25, 1987 (in Icelandic), *Skjálftabréf nr. 65,* pp. 5–9, Sci. Inst. and Icelandic Meteorol. Off., Reykjavík, 1988.

Einarsson, P., and J. Eiríksson, Earthquake fractures in the districts Land and Rangárvellir in the South Iceland Seismic Zone, *Jökull, 32,* 113–120, 1982.

Einarsson, P., and K. Sæmundsson, Earthquake epicenters 1982–1985 and volcanic systems in Iceland (map), in *"Í hlutarins edli", Festschrift for Thorbjörn Sigurgeirsson,* edited by Th. Sigfússon, Menningarsjódur, Reykjavík, 1987.

Einarsson, P., S. Björnsson, G. Foulger, R. Stefánsson, and Th. Skaftadóttir, Seismicity pattern in the South Iceland Seismic Zone, in *Earthquake Prediction: An International Review,* edited by D. Simpson and P.G. Richards, *Maurice Ewing Series* vol. 4, pp. 141–151, AGU, Washington, D.C., 1981.

Ekström G., and E. R. Engdahl, Earthquake source parameters and stress distribution in the Adak Island region of the Central Aleutian Islands, Alaska, *J. Geophys. Res., 94,* 15,499–15,519, 1989.

Eshelby, J. D., The determination of the elastic field of an ellipsoidal inclusion and related problems, *Proc. R. Soc. London, Ser. A, 241,* 376–396, 1957.

Futterman, W. I., Dispersive body waves, *J. Geophys. Res., 67,* 5279–5291, 1962.

Gebrande, H., H. Miller, and P. Einarsson, Seismic structure of Iceland along RRISP-profile I, *J. Geophys., 47,* 239–249, 1980.

Grönvold, K., G. Larsen, P. Einarsson, S. Thórarinsson, and K. Sæmundsson, The Hekla eruption 1980–1981, *Bull. Volcanol., 46(4),* 349–363, 1983.

Halldórsson, P., R. Stefánsson, P. Einarsson, and S. Björnsson, Mat á jardskjálftahættu: Dysnes, Geldinganes, Helguvík, Vatnsleysuvík, Vogastapi og Thorlákshöfn, 34 pp., Stadarvalsnefnd um idnrekstur, Idnadarráduneytid, Reykjavík, 1984.

Hanks, T. C., and H. Kanamori, A moment magnitude scale, *J. Geophys. Res., 84,* 2348–2350, 1979.

Huang, P. Y., Focal depths and mechanisms of mid-ocean ridge

earthquakes from body wave form inversion, Ph.D. thesis, 301 pp., Mass. Inst. of Technol., Cambridge, 1985.

Huang, P. Y., S. C. Solomon, E. A. Bergman, and J. L. Nábělek, Focal depths and mechanisms of Mid-Atlantic Ridge earthquakes from body wave form inversion, *J. Geophys. Res., 91,* 579–598, 1986.

Jakobsson, S.P., Petrology of Recent basalts of the eastern volcanic zone, Iceland, *Acta Nat. Island., 26,* 103 pp., 1979.

Kanamori, H., and C. Allen, Earthquake repeat time and average stress drop, in *Earthquake Source Mechanics, Geophys. Monogr. Ser.,* vol. 37, edited by S. Das, J. Boatwright, and C. Scholz, pp. 227–236, AGU, Washington, D.C., 1986.

Kanamori, H., and D. L. Anderson, Theoretical basis of some empirical relations in seismology, *Bull. Seismol. Soc. Am., 65,* 1073–1095, 1975.

Kárnik, V., *Seismicity of the European Area,* vol. 1, D. Reidel, Hingham Mass., 1969.

Klein, F. W., Hypocenter location program HYPOINVERSE, *U.S. Geol. Surv. Open File Report 78–694,* 113 pp., 1978.

Nábělek, J. L., Determination of earthquake source parameters from inversion of body waves, Ph.D. thesis, Mass. Inst. of Technol., Cambridge, 1984.

Nábělek, J. L., Geometry and mechanism of faulting of the 1980 El Asnan, Algeria, earthquake from inversion of teleseismic body waves and comparison with field observations, *J. Geophys. Res., 90,* 12,713–12,728, 1985.

Ryan, M. P., Neutral buoyancy and the mechanical evolution of magmatic systems, Magmatic Processes: Physiochemical Principles, edited by B. O. Mysen, *Spec. Publ. Geochem. Soc., 1,* 259–287, 1987.

Sæmundsson, K., Evolution of the axial rifting zone in northern Iceland and the Tjörnes fracture zone, *Geol. Soc. Am. Bull., 85,* 495–504, 1974.

Sæmundsson, K., Fissure swarms and central volcanoes of the neovolcanic zones of Iceland, *Geol. J., 10,* 415–432, 1978.

Scholz, C., C. A. Aviles, and S. G. Wesnousky, Scaling differences between large interplate and intraplate earthquakes, *Bull. Seismol. Soc. Am., 76,* 65–70, 1986.

Ward, P. L., New interpretation of the geology of Iceland, *Geol. Soc. Am. Bull., 82,* 2991–3012, 1971.

Wesnousky, S. G., Seismological and structural evolution of strike-slip faults, *Nature, 335,* 340–343, 1988.

I. Th. Bjarnason, Lamont-Doherty Geological Observatory, Palisades, NY 10964.

P. Einarsson, Science Institute, University of Iceland, 107-Reykjavík, Iceland

(Received July 12, 1989;
revised February 23, 1990;
accepted March 22, 1990.)